ELSEVIER

Materials Science and Engineering B 126 (2006) 267–270

MATERIALS SCIENCE & ENGINEERING B

www.elsevier.com/locate/mseb

High frequency magnetic eigen excitations in a spin valve submitted to CPP DC current

Q. Mistral [a,*], A. Deac [b], J. Grollier [a], O. Redon [b], Y. Liu [c], M. Li [c], P. Wang [c], B. Dieny [b], T. Devolder [a]

[a] *Institut d'Electronique Fondamentale, CNRS UMR 8622, Bât 220, Université Paris-Sud, Centre d'Orsay, F91405 Orsay Cedex, France*
[b] *SPINTEC, URA CEA/CNRS, CEA Grenoble/DRFMC, 17 Rue des Martyrs, 38054 Grenoble Cedex 9, France*
[c] *Headway, 678 Hillview Dr., Milpitas, CA 95035, USA*

Abstract

We study the magnetization dynamics induced at low field by spin-transfer in a pillar-shaped spin valve. The spin valve is a square of 150 nm × 150 nm patterned from a film of IrMn 7 nm/CoFe, 2.4 nm/Ru, 0.8 nm/CoFe, 4.4 nm/Cu, 2.6 nm/CoFe, and 3.6 nm. The spin valve is studied in its anti-parallel state at 50 K. The high frequency voltage noise generated by the DC current flowing through the magneto-resistive device is used to identify the excitations induced by spin-transfer. Between an instability current of 1.72 mA and the switching current of 1.89 mA, we demonstrate the existence of pre-switch steady-state excitations, i.e. low amplitude precession. We study the frequency (10 GHz, red shift −1.46 GHz/mA) of this excitation, its line width (78–246 MHz), the power it carries (113 nW), and the current dependance thereof. We discuss those experimental findings using the formalism of Sun et al. and Valet et al., and show that the experimental behavior can be described by a macrospin approximation only at the very onset of the pre-switch excitations. The early saturation of the excitation power and the non-monotonic switching probability with the current are experimental indications that the pre-switch excitations are strongly non-uniform when approaching the switching current.

Keywords: Magnetism; Spin torque; High frequency; Oscillator

1. Introduction

In 1996, Slonczewski [1] and Berger [2] have predicted that a spin polarized current could transfer spin momentum to a magnetization and create a so-called spin transfer torque (STT). A major consequence is that the magnetizations of the layers of a current perpendicular to plane (CPP) giant magneto-resistance (GMR) structure can be manipulated by a current. The back and forth switching was, for instance, observed experimentally in pseudo spin valve nanopillars [3,8], with foreseen interest for bit writing in future magnetic random (MRAM) access.

In addition to switching, STT can also trigger a variety of steady-state precessions in pillar-shaped spin valves when strong magnetic fields and DC currents are applied to the system [4–6]. The precessions arise from a competition between the Zeeman torque and the STT. Of gyromagnetic character, these precessions have frequencies in the range of tens of GHz. So far, most works have focused on the high field and high current regime.

The voltage drop across a STT device partly comes from the GMR effect of structure: the resistivity depends on the relative orientation of the two magnetic layers while the current is kept constant. When this orientation oscillates thanks to precession, a microwave voltage is emitted. Simple models like zero temperature macrospin approximation [7] can account for the field and current needed for the onset of dynamical states. They also describe well their precession frequency. However,they cannot account for the finite line width of the emitted microwave voltage. Quantitative agreement with micromagnetic models is also not complete [11].

In contrast to the published results done with high-applied magnetic fields, we present here magnetization dynamics measurements on a single spin valve device in the specific case of eigen excitations when the applied magnetic field is almost zero. Our measurements are done at 50 K.

2. Experimental

The device considered here was processed [9] from a spin valve film of composition: IrMn 7/P2, 2.4/Ru, 0.8/P1, 4.4/Cu, 2.6/F and 3.6/Ta (thicknesses are in nm). P1 is the pinned layer,

* Corresponding author. Tel.: +33 1 69 15 40 13; fax: +33 1 69 15 78 41.
E-mail address: mistral@ief.u-psud.fr (Q. Mistral).

0921-5107/$ – see front matter © 2005 Elsevier B.V. All rights reserved.
doi:10.1016/j.mseb.2005.09.049

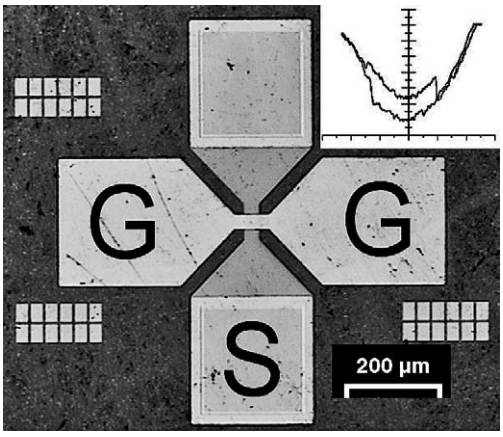

Fig. 1. Optical micrograph of the device. The top electrode is connected using grounded pads (G) while the bottom electrode (S) is used to inject the DC current and extract the RF voltage signal. The pillar is in the middle of the central crossing of the pad-to-electrode stripes. Inset: resistance (7 Ω, MR = 0.15 Ω) vs. current hysteresis loop (switching at −2.67 and 1.9 mA) in zero applied field.

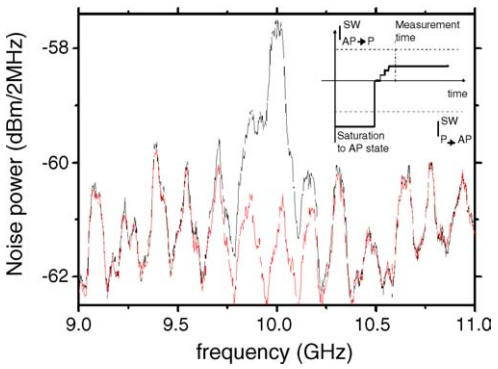

Fig. 2. Representative noise spectra (row data) for two different applied DC currents. The solid line (respectively dashed line) curve corresponds to I_{applied} = 1.79 mA (respectively 0 mA). Inset: illustration of the experimental procedure: the sample is first prepared in the AP state, then the current is ramped to I_{applied} and the noise spectrum is recorded.

P2 is the reference layer, and F is the free layer. F, P1 and P2 are CoFe thin films laminated with copper. The lamination increases both the resistance and the magneto-resistance (MR).

The spin-valve was patterned into a nanopillar of square section of typical size 150 nm, as described in [9]. The pillar is connected in CPP geometry. The resistance of the parallel state is 7 Ω, and its GMR is 150 mΩ (inset in Fig. 1).

The pillar is inserted in a high frequency electrical circuit of bandwidth higher than 18 GHz (Fig. 1). The top electrode is short-circuited to ground pads (G). Current is injected through the bottom electrode (S) using a microwave probe.

The switching currents are $I^{\text{AP}\to\text{P}}_{\text{switching}} = 1.9 \pm 0.06$ mA (8.4×10^6 A cm^{-2}) and $I^{\text{P}\to\text{AP}}_{\text{switching}} = -2.67 \pm 0.15$ mA (-1.19×10^7 A cm^{-2}) at 50 K. For this type of device, a bi-stable hysteretic behavior is observed when the applied field follows $-50\,\text{Oe} < H < 100\,\text{Oe}$. More detailed stability diagrams of switching current versus external magnetic field are gathered in [9].

Our measurement set-up [6] allows to feed a DC current in the sample, to measure its quasi-static resistance and to extract the RF voltage across the sample. The RF voltage is routed through high frequency cables, then amplified and finally analyzed with a 26 GHz bandwidth spectrum analyzer. Since the sample impedance (7 Ω) is not matched to the characteristic impedance of the amplification chain 50 Ω, the amplification gain has a ripple-like small frequency dependence (see Fig. 3) related to voltage standing waves between the sample and the amplifier. The amplification is 45 dB (with a ±1.5 dB ripple) between 100 MHz and 18 GHz. When the resolution bandwidth and the video bandwidth of the spectrum analyzer are set to 2 MHz and 10 kHz, the noise floor the measurement system is 62.5 ± 1.5 dBm, which corresponds to a mean noise floor of −107.5 dBm before amplification, not much above the thermal Johnson noise evaluated to be −111 dBm.

We have measured the RF noise with applied DC currents in the bistable region of the stability diagram. The magnetic field is applied along the easy axis, with a magnitude of 2.1 mT chosen to compensate the dipolar field generated by the pinned and reference layers onto the free layer. Before each measurement, a strong current −10 mA (4.4×10^7 A cm^{-2}) is first applied to prepare the sample in the AP configuration. The applied current is then ramped to I_{applied}, with $0\,\text{mA} < I_{\text{applied}} < 2\,\text{mA}$ (see Fig. 3). Finally the noise spectrum is recorded. In Fig. 3, the dashed curve was measured using this procedure, for a DC current of $I_{\text{applied}} = 0$ mA.

The solid line in Fig. 3 presents a typical row data noise spectrum. A clear signal is detected around 10 GHz. We have systematically checked whether there was some signal at subharmonics (i.e. in the range 4–5.5 GHz) and at harmonics (i.e. in the range 18–20 GHz). No such signal was ever found. To extract the noise power emitted as a result of STT driven precessions, we have treated our row data using Eq. (1).

$$P\,(\text{mW}) = 10^{P_{\text{dBm mes}}/10} - 10^{P_{\text{dBm ref}}/10} \tag{1}$$

where $P_{\text{dBm mes}}$ is the row data noise power density at I_{applied} and $P_{\text{dBm ref}}$ is the reference noise power density, i.e. at $I = 0$ mA.

A representative noise power is displayed in Fig. 3. Power is emitted around a frequency of 10 GHz. This frequency of emission diminishes (i.e. red shift) with increasing current. On the noise spectra, there are some positive spikes (9.23, 9.55, and 10.94 GHz) and negative spikes (10.26, 10.59 GHz) that do not shift with the applied current. As it is illustrated in Figs. 2 and 3 by the vertical dashed lines, these extrema correspond to minima in the amplification gain. At these points, the signal crosses the noise floor and the treatment of Eq. (1) fails to provide the true noise spectrum.

3. Results

RF emission was observed for applied currents above a current defined as the instability current $I^{\text{AP}\to\text{P}}_{\text{instability}} = 1.72 \pm 0.01$ mA, provided that the sample was still in the AP state when the noise spectrum was recorded. The system has always switched when the applied current exceeds $I^{\text{AP}\to\text{P}}_{\text{switching}} = 1.9$ mA. Note that contrary to what could be expected, the probability of switching during the measurement duration was not monotonic

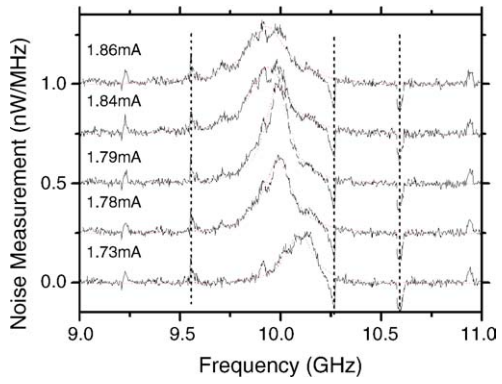

Fig. 3. Noise spectra after correction of the amplification gain ripple by subtraction of the reference noise in the remanent AP state. The displayed spectra are recorded while the sample is in the AP state. They are shifted vertically by integer increments of 0.5 fW/Hz.

with the applied current in the interval $I_{\text{instability}}^{\text{AP}\to\text{P}} < I_{\text{applied}} < I_{\text{switching}}^{\text{AP}\to\text{P}}$. This switching probability was maximum and very high in the interval 1.73–1.78 mA, and no spectrum could be recorded in that applied current interval (see Fig. 4c). Surprisingly, the switching probability was smaller at higher applied currents, and noise spectra could be recorded up to $I_{\text{switching}}^{\text{AP}\to\text{P}}$.

We have fitted the experimental noise spectra with a Lorentzian functions to get the central emission frequency, the line width and the total emitted power (Fig. 4).

At $I_{\text{instability}}$, the central emission frequency is 10.16 GHz. When the applied current is increased, the central emission frequency red shifts at a rate of $-1.46\,\text{GHz}\,\text{mA}^{-1}$.

In the interval $I_{\text{instability}}^{\text{AP}\to\text{P}} < I_{\text{applied}} < I_{\text{switching}}^{\text{AP}\to\text{P}}$, the line width of the microwave noise power grows significantly from 78 to 246 MHz. The noise maximum amplitude first increases until the applied current reaches 1.79 mA ($7.96 \times 10^6\,\text{A}\,\text{cm}^{-2}$), and then decreases. As a result, the total power emitted by the device

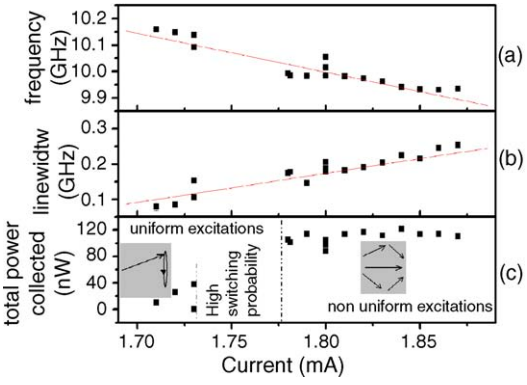

Fig. 4. Evolution of the frequency of emission vs. current (a), line width vs. current (b) and total power collected (c). The absence of data points between 1.71 and 1.77 mA recalls that in this current interval the switching probability was near 1 during the typical acquisition time, such that no AP state spectrum could be recorded. Light lines in (a) and (b) are linear fits of the data: $f\,(\text{GHz}) = 12.6–1.5I\,(\text{mA})$ for (a) and $w\,(\text{GHz}) = -1.32 + 0.83I\,(\text{mA})$ for (b). Inset in (c): illustration of the proposed excitation scenario: below 1.71 mA the excitation is spatially uniform, while there is spatial non-uniformity when approaching the switching current.

(Fig. 4c) first increases linearly until $I_{\text{applied}} = 1.79$ mA and then saturates to the value 113 nW.

4. Discussion

The existence of distinct instability and switching currents was already predicted by Sun [7] and was recently experimentaly observed by Kiselev et al. and Devolder et al. [4,6].

The instability current density has been calculated by Katine et al. [3] for a macrospin at zero temperature. It is (Eq. (2)):

$$j_{\text{instability}}^{\text{AP}\to\text{P/P}\to\text{AP}} = \frac{\pm e\alpha M_s t_1((Hd/2) + Hk)}{\hbar P_{\text{eff}}} \tag{2}$$

where P_{eff} is the effective spin polarization, t_1 is the free layer thickness and α is the damping factor.

Note that at this instability current, the P state becomes linearly unstable while the AP state is stable. This does not imply that the system will switch from P to AP; it only implies that the system must exit from the P configuration. Sun [7] has shown theoretically that the magnetization of the free layer enters a dynamical state which is a precession along an elliptic cone about the easy axis. This cone has an in-plane aperture which grows continuously with the current density. When this angle reaches 180°, the magnetization overcomes the hard axis and switches irreversibly to the AP state at $I_{\text{switching}}$ [6]. Grollier et al. [8] have calculated the frequency of precession at $I_{\text{instability}}$. At first order, this frequency is (Eq. (3)):

$$f = \frac{\gamma_0}{2\pi}\sqrt{HkM_s} \tag{3}$$

when $\gamma_0 = 2.21 \times 10^5\,\text{H}\,\text{m}\,\text{A}^{-1}$. From this frequency and [9] $M_s = 0.95\,10^6\,\text{A}\,\text{m}^{-1}$, we evaluate the anisotropy to be 106 mT.

Recently, Valet [10] has developed an analytical estimate of the switching current. He has assumed (i) a macrospin behavior; (ii) zero temperature; and (iii) that the STT prefactor that can be expressed as $P_{\text{eff}} = \frac{\eta_0}{1\pm\beta}$, where η_0 is a spin polarization factor, β is a measurement of the asymmetry of spin polarization between the AP and P configurations, and '±' is '+' for P configuration and '−' for the AP configuration.

At zero applied field, Valet's switching current density is (Eq. (4)):

$$j_{\text{switching}}^{\text{AP}\to\text{P/P}\to\text{AP}} = \frac{\pm\alpha M_s^2\, t_1\, e}{\hbar\eta_0}\,\frac{\sqrt{1-\beta^2}}{\arctan(\sqrt{(1-\beta)/(1+\beta)})} \tag{4}$$

where ± is "+" for the AP → P and "−" for P → AP.

Let us now discuss our experimental instability and switching currents in the framework of the above-mentioned models, assuming first a macrospin behavior. Using the approximation that $I_{\text{instability}}^{\text{P}\to\text{AP}} \approx I_{\text{switching}}^{\text{P}\to\text{AP}}$, we can extract β from the ratio of the P → AP to AP → P instability currents. The experimental data yield $\beta = +0.16$. Note that this value indicates that the electronic transport is mostly diffusive in our system, since the purely ballistic transport approximation [1] would yield $\beta > 1/3$.

Once we know β, we can use the instability currents to estimate the ratio of spin polarization to damping parameter. We find that $\alpha/\eta_0 \approx 0.02$. This value is consistent with a spin polarization of $\eta_0 \approx 0.3$ and a damping parameter of $\alpha = 0.007$.

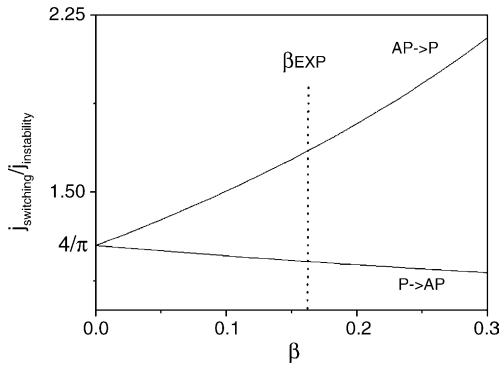

Fig. 5. Ratio of the switching current (Eq. (3)) to the instability current (Eq. (2)) and its dependence to the spin-transfer switching currents asymmetry coefficient β.

According to Valet's model, the ratio of the switching to the instability current is a sole function of β and of the state (AP or P) the system is in. The expected dependence of $j_{switching}/j_{instability}$ versus β is displayed in Fig. 5. Note that according to this model, the interval $[j_{switching}; j_{instability}]$ where pre-switch excitations exist is much broader near the AP $\rightarrow$ P transition than near the P $\rightarrow$ AP transition. This renders easier the experimental detection of the dynamical state around the AP to P transition, as has been done in the present study. However, the experimental β value would yield an expected $j_{switching}/j_{instability} = 1.66$, while the experimental ratio is only 1.1.

Clearly, the macrospin approximation cannot describe quantitatively our experimental critical currents. In addition, it can also not explain the saturation of the emitted power above $I = 1.78$ mA (7.9×10^6 A cm^{-2}) (Fig. 4c). Indeed, macrospin models, either at 0 K or at finite temperature, predict a clear increase of emitted power with the current in the interval $[j_{switching}, j_{instability}]$, see [6].

Another argument for the need to take into account some spatial non-uniformity of the free layer magnetization comes from the switching probability. Indeed no data point could be recorded in the range [1.73 mA (7.7×10^6 A cm^{-2}); 1.78 mA (7.9×10^6 A cm^{-2})]. Above 1.78 mA, the pre-switch excitations have a different character since its power saturates. Since the macrospin model (regular increase of power with the current) seems satisfied below 1.78 mA, the free layer magnetization is likely to have a large spatial coherence (see the sketches in Fig. 4c). As the current is increased above 1.73 mA, the excitation amplitude is expected to grow to such an extent that the switching is almost certain during the measurement time.

In the range [1.79 mA (8×10^6 A cm^{-2}); 1.89 mA (8.4×10^6 A cm^{-2})] the measured noise power saturates. This is likely to be due to spatial non-uniformities of the excitation mode. The idea is the following. When the non-uniformities of the excitation mode leads to a phase difference of π between the instantaneous excitation amplitudes at two places inside the free layer (see the sketches in Fig. 4c), the corresponding local magneto-resistance voltages interfere destructively, which degrades the measured noise power. As a result, any departure from the macrospin behavior decreases the experimental signature of the excitation, i.e. the noise power.

5. Conclusion

We have studied the magnetization dynamics induced by spin-transfer in a pillar-shaped spin valve at nominally zero applied field. The high frequency voltage noise has been used to characterize the excitations induced by spin-transfer. Pre-switch steady-state excitations were observed between an instability current of 1.72 mA and the switching current of 1.89 mA. They are low amplitude precession, of frequency 10 GHz and line width 78–246 MHz). The experimental behavior can be described by a macrospin approximation only at the very onset of the pre-switch excitations. The saturation of the excitation power and the non-monotonic switching probability with the current are experimental indications that the pre-switch excitations are strongly non-uniform when approaching the switching current.

References

[1] J.C. Slonczewski, J. Magn. Magn. Mater. 159 (1996) L1.
[2] L. Berger, Phys. Rev. B 5 (1996) 9353.
[3] J.A. Katine, et al., Phys. Rev. Lett. 84 (2000) 3129.
[4] S.I. Kiselev, et al., Nature (London) 25 (2003) 380.
[5] W.H. Rippard, et al., Phys. Rev. Lett. 92 (2004) 027201.
[6] T. Devolder, et al., Phys. Rev. B 71 (2005) 184401.
[7] J. Sun, Phys. Rev. B 62 (2000) 570.
[8] J. Grollier, et al., Phys. Rev. B 67 (2003) 174402.
[9] A. Deac, et al., J. Magn. Magn. Mater. 290–291 (2005) 42–47.
[10] T. Valet, to be published.
[11] D.V. Berkov, et al., CondMat 0503754v2, to be published.